Experimental Eye Research 240 (2024) 109815

Contents lists available at ScienceDirect

Experimental Eye Research

journal homepage: www.elsevier.com/locate/yexer

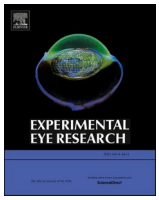

Research article

Impact of culture media on primary human corneal endothelial cells derived from old donors

Alessia Merra [a,b], Eleonora Maurizi [b,*], Graziella Pellegrini [a,b]

[a] Holostem Terapie Avanzate S.r.l., Modena, Italy
[b] Centre for Regenerative Medicine, University of Modena and Reggio Emilia, Modena, Italy

ARTICLE INFO

Keywords:
Primary human corneal endothelial cells
Old donor corneas
Cell culture
Cell therapy
Regenerative biology

ABSTRACT

Corneal endothelial dysfunction is a major indication for corneal transplantation. However, a global shortage of donor corneal tissues and risks associated with corneal surgeries have prompted exploration of alternative options, including tissue-engineered grafts or cell injection therapy. Nonetheless, these approaches require a controlled culture of primary human corneal endothelial cells (HCEnCs). Although HCEnCs established from young donors are generally more proliferative and maintain a better phenotype, corneas from old donors are more frequently accessible from eye banks due to a lower corneal endothelial cell count than the necessary threshold required for transplantation.

In this study, we investigated various culture media to evaluate which one is the most appropriate for stimulating the proliferation while maintaining cell morphology and function of HCEnCs derived from old donors (age >65 years). All experiments were performed on paired research-grade donor corneas, divided for the conditions under investigation in order to minimize the inter-donor variability. Cell morphology as well as expression of specific markers were assessed at both mRNA (CD166, SLC4A11, ATP1A1, COL8A1, α-SMA, CD44, COL1A1, CDKN2A, LAP2A and LAP2B) and protein (ZO-1, α-SMA, Ki67 and LAP2) levels. Results obtained showed how the Dual Media formulation maintained the hexagonal phenotype more efficiently than Single Medium, but cell size gradually increased with passages. In contrast, the Single Medium provided a higher proliferation rate and a prolonged *in vitro* expansion but acquired an elongated morphology.

To summarize, Single medium and Dual media preserve morphology and functional phenotype of HCEnCs from old donor corneas at low passages while maintenance of the same cell features at high passages remains an active area of research. The new insights revealed within this work become particularly relevant considering that the elderly population a) is the main target of corneal endothelial therapy, b) represents the majority of corneal donors. Therefore, the proper expansion of HCEnCs from old donors is essential to develop novel personalised therapeutic strategies and reduce requirement of human corneal tissues globally.

1. Introduction

The corneal endothelium (CE) and its basal membrane (the Descemet's membrane) are the innermost layers of the cornea, located between the corneal stroma and the anterior chamber. The "barrier and pump" functions of the CE preserve the dynamic regulation of the corneal hydration, crucial for maintaining corneal transparency (Maurice, 1957). In spite of the commonly used terminology, the CE is most probably not a true endothelial layer but rather a specialized epithelial layer (Shamsuddin et al., 1986). However, unlike other types of epithelial cells (Maurizi et al., 2021), human corneal endothelial cells (HCEnCs) exhibit nearly complete inhibition of spontaneous proliferation *in vivo* (Joyce, 2012) although there are some interventions that appear to trigger this capacity (Galvis et al., 2013). Thus, in the conditions of non-intervention with these new approaches, HCEnCs loss related to aging or disease is compensated by migration and enlargement of the neighbouring cells (Joyce, 2003). However, when the endothelial cell density falls below the critical threshold of approximately 500 cells/mm^2, this mechanism fails to maintain the corneal hydration state. Subsequently, corneal oedema occurs, leading to corneal opacity and visual impairment (Mimura et al., 2013; Mishima, 1982). To date, the most commonly utilized and effective treatment for

* Corresponding author.
E-mail address: eleonora.maurizi@unimore.it (E. Maurizi).

https://doi.org/10.1016/j.exer.2024.109815
Received 18 October 2023; Received in revised form 18 December 2023; Accepted 29 January 2024
Available online 3 February 2024

corneal endothelial dysfunctions is corneal transplantation, specifically posterior lamellar grafts developed over the past two decades, such as DSAEK and DMEK. These techniques are considered safer and allow for faster recovery compared to penetrating keratoplasty (Hemaya et al., 2023; Musa and Zeppieri, 2023; Nanavaty et al., 2014). Despite their high success rates, these procedures are technically complex and come with inherent risks, including the potential for primary graft failure and immune rejection (Galvis et al., 2017; Romano et al., 2023; van Essen et al., 2015) Moreover, the global shortage of donor corneas has become a significant concern, with only one cornea available for every 70 needed (Gain et al., 2016). Newer surgical options that do not require allogeneic grafts, such as Descemet stripping only (DSO), have shown promising results. However, the relatively low final cell densities achieved with DSO make these techniques not yet widely adopted (Davies et al., 2021). The investigation of alternative strategies for treating corneal endothelial impairments is therefore crucial for developing innovative therapeutic solutions. It has been known for more than five decades that HCEnCs have *in vitro* proliferation potential under appropriate conditions (Baum et al., 1979). Tissue engineering approaches, such as the intracameral injection of HCEnCs, have shown promising initial results in medium-term human follow-ups (Numa et al., 2021). However, these approaches require the establishment of a consistent cell culture protocol for HCEnCs, necessitating the fine-tuning of all involved procedures (Wongvisavavit et al., 2021).

In 1979, the first HCEnCs mass culture was described (Baum et al., 1979). Over the next decades, several culture media have been reported with numerous combinations of minimal essential media (Bartakova et al., 2018; Choi et al., 2014; Ishino et al., 2004; Jäckel et al., 2011; Parekh et al., 2019b; Peh et al., 2011b), enriched for Fetal Calf Serum (FCS) or Fetal Bovine Serum (FBS) and additional components (such as insulin, transferrin, hypoxanthine, thymidine, ascorbic acid, calcium chloride, chondroitin sulphate), growth factors (Beaulieu Leclerc et al., 2018; Joyce et al., 1989; Lee et al., 2012; Li et al., 2005), and small molecules (Okumura et al., 2013, 2017). Successful expansion of HCEnCs represents a balance between the intended stimulation of cell proliferation and the undesired induction of premature cell senescence and Endothelial-to-Mesenchymal Transition (EnMT). The EnMT involves the progressive loss of CE hallmarks and contemporary acquisition of mesenchymal characteristics, such as disassembly of cell–cell junctions, loss of apical–basal polarity, actin cytoskeleton reorganisation, increased cell motility and proliferation, increased production of extracellular matrix (ECM) proteins and loss of CE functions (Lamouille et al., 2014; Roy et al., 2015b). At low passages *in vitro*, HCEnCs form a contact-inhibited monolayer of polygonal-shaped cells that express cell junction proteins such as ZO-1 and N-cadherin and markers associated with HCEnCs functionality such as Na^+K^+/ATPase and SLC4A11 (Chng et al., 2013; Frausto et al., 2020; He et al., 2016). However, as the passages increase, HCEnCs change their cell shape, lose contact inhibition and express characteristic EnMT markers (α-SMA, CD44, etc.) (Hamuro et al., 2016b; Roy et al., 2015a). Triggering factors leading to EnMT impact critical intracellular pathways, such as TGF-β/Smad and TGF-β/non-Smad signalling, canonical Wnt/β-catenin signalling, PI3K–AKT and ERK-MAPK activation by growth factors, or Notch signalling (Li et al., 2013; Maurizi et al., 2020; Roy et al., 2015a; Zhu et al., 2012). Novel culture media supplements involve inhibitors of these signalling pathways that significantly improve the HCEnCs cultures outcome. For example, TGF-β pathway could be inhibited by treating HCEnCs with SB-431542 or LY-2109761 (Okumura et al., 2013; Zhang et al., 2018). Recently, we proposed the use of CHIR99021 (a GSK-3 Inhibitor) to revert the EnMT that physiologically occurs in primary HCEnCs culture of old donors (Maurizi et al., 2023). Other small molecules used to promote the propagation of isolated primary HCEnCs are ROCK inhibitors that increase cellular adherence and proliferation while maintaining cell morphology (Okumura et al., 2011a, 2011b, 2014b; Peh et al., 2015a; Pipparelli et al., 2013). However, some studies found that the most used ROCK inhibitor, Y-27632, did not stimulate HCEnCs proliferation but confirmed its positive impact on CE healing (Bartakova et al., 2018; Pipparelli et al., 2013). The effects of ROCK inhibitors on HCEnCs appear therefore to depend on the cell source and culture conditions. Furthermore, Y-27632 showed to have an effect in increasing HCEnCs proliferation and adhesion exclusively in cultures derived from young donors, as the addition of the ROCK inhibitor was not found to be advantageous for cultures established by old donor corneas (Peh et al., 2015a; Pipparelli et al., 2013). Up to date, two of the main strategies used for primary HCEnCs *in vitro* expansion are either a Single medium (Engelmann et al., 1988; Okumura et al., 2013) or Dual media (Peh et al., 2015b). The former is a mitogenic-rich medium based on the medium used in the first-in-human clinical trial in 2018 (Kinoshita et al., 2018) while the Dual media method alternates a mitogenic medium during cell growth, and a maintenance medium when HCEnCs reach confluency (Peh et al., 2015b).

Donor characteristics such as age, post-mortem time, cause of death, cell density, background diseases, pre-death drug use, and graft storage conditions can significantly influence the success of cell culture (Català et al., 2022; Choi et al., 2014; He et al., 2011; Konomi et al., 2005; Krohn and Høvding, 2005; Lass et al., 2019; Peh et al., 2011a; Redbrake et al., 1994). HCEnCs derived from young donors (<30 years old) show better adherence to the culture substrate, a higher *in vitro* proliferation rate, and they can reach a greater number of passages without chromosomal aberrations (Joyce and Zhu, 2004; Konomi et al., 2005; Miyata et al., 2001; Senoo and Joyce, 2000; Ting et al., 2022; Zhu and Joyce, 2004). On the other hand, HCEnCs derived from old donor corneas (>50 years old) have a limited proliferative ability (Enomoto et al., 2006) and present a senescent phenotype with truncated telomeres and damaged DNA due to oxidative stress, which is induced by high HCEnCs metabolism rates and ultraviolet (UV) light (Joyce et al., 2009, 2011), as also observed in other corneal pathologies (Cullen, 2002; Maurizi et al., 2019). For these reasons, most of the current culture protocols include isolation of HCEnCs from young donors (Frausto et al., 2020; Kinoshita et al., 2018; Miyata et al., 2001; Peh et al., 2015b). However, although primary HCEnCs established from young donors are more easily expanded *in vitro*, old donor tissues (i.e., above 65 years of age) are more frequently available for research since they present a lower density than the threshold required for transplantation. Moreover, studying HCEnCs from old donor corneas is more representative of the main therapeutic target requiring corneal endothelial transplatation. Nevertheless, culturing cells from old aged donors is far more challenging, and no protocol specifically designed for their clinical application has been established so far. It is therefore essential to compare existing culture systems to determine their efficiency in supporting a long-term culture of HCEnCs from old donors. Herein, we investigated different culture media (Kinoshita et al., 2018; Peh et al., 2015b) to evaluate which one is the most appropriate for stimulating the *in vitro* proliferation of HCEnCs from old donors while maintaining their morphology and function. These studies were performed on paired donor corneas divided for the conditions studied, in order to minimize the inter-donor variability. HCEnCs were expanded *in vitro* and morphology as well as CE markers at both mRNA and protein levels were examined, in Single and Dual culture media conditions. This work gives new insights into HCEnCs culture from old donor corneas and new perspectives for reducing the requirement of human corneal tissues globally.

2. Materials and methods

2.1. Ethical statement

Human donor corneas, unsuitable for transplantation, were procured by Veneto Eye Bank Foundation (FBOV) with written informed consent for research use from donor's next of kin. The experimental protocol was approved by ISS- CNT (Italian National Transplant Centre). The research protocol on human corneal tissues was approved by the local ethical committee (Comitato Etico dell' Area Vasta Emilia Nord, p. 0002956/

20). The tissues were handled in accordance with the declaration of Helsinki.

2.2. Primary HCEnCs harvesting and culture

Research-grade human corneal tissues were preserved in Eusol-C (CSM 001-00, Alchimia s.r.l.) at 4 °C and used within 15 days from the donor's death. A list of details for each cornea used and relative experiments is shown in Table 1. Each biopsy was subject to mycoplasma test (MycoAlert® Mycoplasma Detection Kit), assayed at the GloMax® Multi Detection System with Instinct ™ Software. Each biopsy was treated under sterile condition. Corneas were washed three times in sterile Dulbecco's phosphate buffered saline (DPBS, Gibco) added with 2 % of antibiotic/antimycotic solution for 10 min (min) each. Primary HCEnCs were isolated using a two-step, peel and digest method. Specifically, corneoscleral rims were placed endothelial side up on a dish. A brief 30 s (s) incubation with Trypan Blue solution 0.1 % (Sigma-Aldrich) was used prior to stripping off the DM-endothelial layer under the stereomicroscope (ZEISS Stemi DV4 Stereo Microscope). Paired DM-endothelial layers obtained were pooled and digested enzymatically in 1.5 mg/mL Collagenase A (Roche Diagnostic) for approximately 3 h (h) at 37 °C. HCEnCs clusters isolated from DM were further dissociated by TryPLE (Thermo Fisher Scientific) for 5 min at 37 °C and the resulting smaller clamps were plated ($2.1 \times 10^4/cm^2$) in wells treated with 50 μg/mL Laminin511 (BioLamina). HCEnCs were cultured at 37 °C under 95/5 % air/CO_2 atmosphere, changing the growth medium every other day. Sub-confluent cultures (plated at $0.8 \times 10^4/cm^2$) were harvested 48 h after plating. Growth media used for experiments are described in Table 2. In the Single Medium w/Rock Inhibitor 10 μM Rock Inhibitor Y27632 was added during cell plating. In the Dual Media culture approach, HCEnCs were first established in M5 medium overnight and then cultured in M4 until they reached 90–95 % confluence (approximately 2 weeks), when M5 was reintroduced for 2–4 days before passaging (Peh et al., 2015b). Upon confluency, HCEnCs were rinsed in DPBS and dissociated with TrypLE for 10–15 min at 37 °C in 5 % CO_2.

2.3. Cell morphometry analysis

Cell morphometric analysis was performed using ImageJ software. Morphometric values of cell circularity and area were obtained from phase contrast images of the culture at confluence by manually outlined point-to-point each cell borders (Schneider et al., 2012). A value approaching 1.0 is equivalent to a cell with a cellular profile closer to a perfect circle. Therefore, hexagonal HCEnCs will have a profile next to 1.0, whereas elongated fibroblast-like HCEnCs will have a circularity value closer to zero (Peh et al., 2012). An average of 50 cells for each condition were analysed, from three different donors each (n = 3, for each experiment).

Table 1
HCEnCs donor information. Primary HCEnCs used for the experiments are all derived from old donors (age above 60 years old). D/P indicates the time (in hours) between death and preservation start of donor human corneas. ECD = corneal endothelial cell density. The blanks (–) indicate that ECD examination was not performed. Columns on the right indicate experiments done for each strain: A: Morphological assessment and growth profile; B: Real-time PCR analysis; C: Immunofluorescence staining; D: FACS analysis.

Serial Number	Age (years)	D/P (hours)	ECD (cells/mm^2)	Experiment			
				A	B	C	D
01	74	19	1800	•		•	
02	72	19	–	•	•	•	
03	67	10	1800	•	•	•	
04	61	5	1900	•	•		
05	67	14	1800	•			
06	69	6	–	•			
07	77	23	1700			•	
08	76	6	1900	•		•	
09	66	20	–			•	
10	79	15	1700			•	
11	73	6	1800			•	
12	69	10	1900			•	
13	78	7	1900	•	•	•	•
14	75	7	1800	•	•	•	•
15	69	16	1800	•	•	•	•
16	73	6	–	•		•	

2.4. Quantitative real time (RT)-PCR

HCEnCs RNA was extracted by RNeasy Plus Micro Kit (Qiagen), quantified with the Nanodrop 100 (Thermo Fisher Scientific) and reverse transcribed into cDNA using the High-Capacity cDNA Reverse Transcription Kit (Thermo Fisher Scientific). RT-PCR assays were performed using 7900HT Fast Real-Time PCR System (Thermo Fisher Scientific). The TaqMan Real Time PCR Assays probes and the primers for SyBr Green are listed Tables 3 and 4. GAPDH was used as housekeeping control and ΔCt calculation was performed to evaluate effective RNA expression. For each condition, all complementary cDNA samples were run in triplicate. Each gene was evaluated in cells deriving from three different donors for each condition (n = 3), in two donors for the Rock Inhibitor analysis (n = 2).

2.5. Immunofluorescence (IF)

Immunofluorescence staining was performed on primary cultured HCEnCs after fixation in 3 % PFA, 15 min at room temperature (RT) or Methanol, 10 min at −20 °C, the latter specifically for Na^+/K^+ ATPase. Triton X-100 (Bio-Rad), used at 1 % for 10 min at RT, allowed cell permeabilization and a solution of bovine serum albumin (BSA; Sigma-Aldrich) 2 %, FBS 2 %, Triton X-100 at 0.01 % in PBS was used for 30 min at 37 °C to block the non-specific binding sites. Primary and secondary antibodies were incubated for 1 h at 37 °C while nuclei were counterstained with DAPI (Roche Diagnostic) at RT for 5 min before mounting the glass coverslips using DAKO mounting medium (Agilent). Primary antibodies used are listed in Table 5 while secondary antibodies used are Alexa Fluor 488 anti-rabbit and Alexa Fluor 488 anti-mouse, 1:2000, and Alexa Fluor 568 anti-mouse and Alexa Fluor 568 anti-rabbit, 1:1000 (Thermo Fisher Scientific). Three rinses in PBS were performed between all steps except before incubation with the primary antibody. Images were obtained with a confocal microscope (LSM900 Airyscan—Carl Zeiss). Quantification of α-SMA, LAP2 and ki67 staining was obtained by counting the number of positive cells (primary antibody signal), relative to the total number of cells in that field (DAPI staining). The values obtained from cells of different donors were expressed in percentage with standard deviation. Six (C, confluent) and ten (S, sub-confluent) fields from three different strains of three different biological experiments were used for quantification (n = 3).

2.6. Cell cycle analysis by flow cytometry (FACS)

The cell cycle was studied by staining sub-confluent cultures of HCEnCs with Propidium Iodide (PI) (Sigma-Aldrich). HCEnCs suspension from cell culture was washed with DPBS and incubated for 1 h at 4 °C in the dark with 250 μL of a PBS solution containing PI 50 μg/mL, Triton X-100 (Bio-Rad) at 0.1 %. After staining, cells were analysed using BD FACS Canto II (BD BIOSCIENCES). For each sample, 20.000 events were counted and considered for the analysis to ensure statistical relevance. Results were analysed with a ModFit 3.0 software.

2.7. Statistical analysis

Microsoft Excel 2010 and GraphPad Prism 5 software were used for data and statistical analysis. Values were represented as mean ± standard deviation (SD). Statistical comparison was done using two-tailed

Table 2
Cell culture media used for the experiments. Composition and references of the four culture media that have been tested on primary HCEnCs derived from old donors: Single Media A, Single Medium B, Single Medium C and Dual Media D. FBS = Fetal Bovine Serum; EGF = Epidermal Growth Factor; ITS = Insulin, transferrin, selenium; p/s = penicillin/streptomycin; bFGF = basic Fibroblast Growth Factor; PMA = Phorbol-12-Myristate-13-Acetate.

	Basal medium	FBS	Growth factors & Supplements	Reference
Single Medium A	DMEM & Ham's F12 (3:1 ratio)	5 %	4 mM Glutamine 50 IU/ml Pen/strep 0.18 mM Adenine 1.1 μM Hydrocortisone 5 μg/ml Insulin 2 nM Triiodothyronine 0.1 nM Cholera toxin 10 ng/ml EGF 1 ng/ml bFGF 10 ng/ml PMA	De Luca et al. (1988)
Single Medium B	DMEM & Ham's F12 (2:1 ratio)	10 %	4 mM Glutamine 50 IU/ml Pen/strep 0.18 mM Adenine 1.1 μM Hydrocortisone 5 μg/ml Insulin 2 nM Triiodothyronine 0.1 nM Cholera toxin 10 ng/ml EGF	Pellegrini et al. (1999)
Single Medium C «Single Medium»	Opti-MEM-I	8 %	5 ng/ml EGF 20 μg/ml ascorbic acid 200 mg/L calcium chloride 50 mg/ml gentamicin 0.5 % antibiotic/antimycotic 0.08 % chondroitin sulphate 10 μM ROCK Inhibitor Y27632	Kinoshita et al. (2018)
Dual Media D "Dual media"	STABILIZATION MEDIUM Human endothelial-SFM PROLIFERATIVE MEDIUM Ham's F12 & M199 (1:1 ratio)	5 % 5 %	1 % antibiotic/antimycotic 20 μg/ml ascorbic acid 1 % ITS 10 ng/ml bFGF 1 % antibiotic/antimycotic	Peh et al., 2015a; 2015b

Table 3
Probes used for the qRT PCR experiments. TaqMan assays were all purchased from Thermo Fisher Scientific.

Gene	Probes
CDKN2A (p16)	Hs00923894_m1
GAPDH	Hs02786624_g1

Table 4
Primers used for the qRT PCR experiments. Primers were all purchased from Macrogen Europe.

Gene	Primers sequence (5′–3′)
GAPDH	F: GTCTCCTCTGACTTCAACAGCG R: ACCACCCTGTTGCTGTAGCCAA
αSMA	F: CCGGGAGAAAATGACTCAAA R: GCAAGGCATAGCCCTCATAG
CD166	F: CCCCAGAGGAATTTTTGTTTTAC R: AGCCTGATGTTATCTTTCATCCA
CD44	F: TCGCTACAGCATCTCTCGGAC R: TTCTCCATCTGGGCCATTGTG
ATP1A1	F: GAAGCTCATCATTGTGGAAGG R: AGTCATTCACACCGTCACCA
COL8A1	F: AGAGGGGAGAAAGGACCAATAG R: CCTACTTCACCAAGGAAACCTG
SLC4A11	F: TGCTCTATGGCCTCTTCCTC R: CCCTCCGGATGTAGTGTGTC
COL1A1	F: TCCAACGAGATCGAGATCC R: AAGCCGAATTCCTGGTCT
LAP2α and β LAP2α LAP2β	F: ATT GTG GGA ACA ACC AGG AA R: CCA CCA GAG GGA GTA GTT C R: TTT GCT CTG CCC TTT AGT GG

Student's t-test, while gene expression data were compared with a Student t-test. Significance was set at $p < 0.05$ and the number of replicates is indicated for each experiment in the relative Figure.

Table 5
Antibodies and relative dilutions used for IF analysis.

Primary Antibodies	Reference	Dilution
ZO-1	40-2200 (ThermoFisher)	1:100
α-SMA	A5228 (Sigma Aldrich)	1:200
Na^+/K^+ ATPase	05-359 (Merck)	1:200
N-cadherin	610920 (BD Biosciences)	1:100
Ki-67	ab15580 (Abcam)	1:50
CK-8	61038 (Progen)	1:200
CK-18	ab7797 (Abcam)	1:200
Pankeratin	C1145455 (Cell Signaling)	1:200
LAP2	611000 (BD Biosciences)	1:100

3. Results

3.1. Donor information

Research-grade human corneal tissues (n = 32) used in these studies were deemed unsuitable for transplantation due to donor characteristics (i.e., positive infectious serological testing) or corneal quality (i.e., ECD <2500 cells/mm^2) (Table 1). Average ECD before HCEnCs isolation was 1816.67 (±71.77) cells/mm^2. The mean age of the cadaveric donors was 71.56 (±4.98) years and the time taken from the donor death to the tissue preservation averaged 11.81 (±6.12) hours. Tissues were preserved at 4 °C less than 15 days from the donor's death.

3.2. Morphology and growth of primary HCEnCs in Single Medium and Dual Media

A total of six pairs of donor corneas (Table 1, serial numbers 01 to 06) were used to compare cells growth in Single Medium and Dual Media (Fig. 1). At low passages, no significant morphological differences were observed between HCEnCs grown in Single medium and Dual media. At confluence, HCEnCs formed a compact monolayer, presenting a general

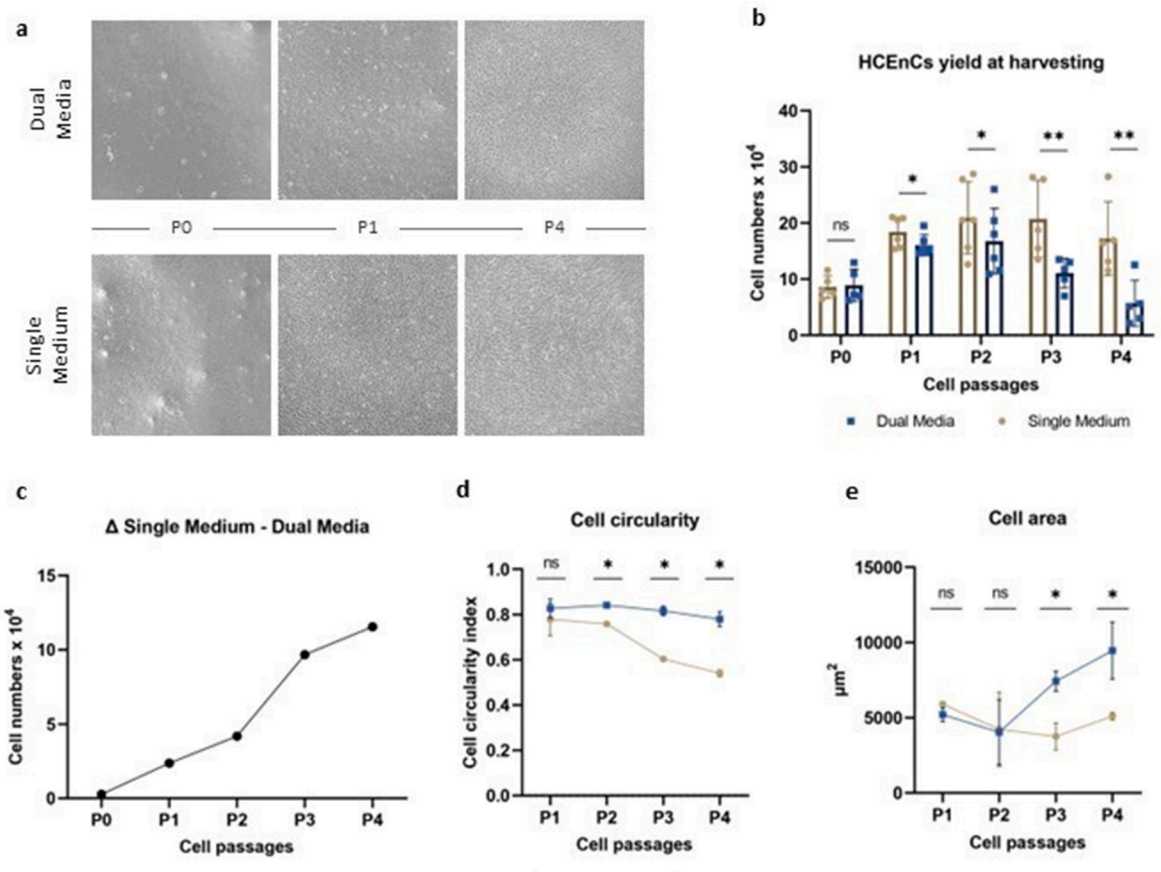

Fig. 1. Morphological assessment and growth profile of HCEnCs in Single Medium and Dual media. a) Representative sets of phase-contrast photomicrographs showing HCEnCs morphology from passage (P) 0 to P 4 (n = 6). b) HCEnCs yield at harvesting from P0 to P4 (n = 6). Total cell numbers are expressed as values ± SD. c) Delta of HCEnCs yield at harvesting between Single Medium and Dual Media conditions, studied across passages (P0 to P4) (n = 6). d) Cell circularity of HCEnCs at subsequent passages in culture at confluence. Cell circularity is expressed as values ± SD (n = 3). e) Cell size of HCEnCs from P1 to P4 at confluence. Quantitative data are expressed as values ± SD (n = 3). Statistical significance was assessed using a Student t-test and set at $p < 0.05$. p values are indicated as following: ns (not significative) when $p > 0.05$, * when $p < 0.05$, ** when $p < 0.01$, *** when $p < 0.001$.

homogeneous cell size and shape in both culture conditions. However, at higher passages (P4), HCEnCs cultured in Dual media appeared more polygonal/hexagonal than their counterparts cultured in Single medium, where HCEnCs showed a typical fibroblast-like morphology (Fig. 1a). The HCEnCs number at harvesting was constantly lower in Dual media than in Single medium, starting from P2 ($p = 0.03$) and increasing progressively until P4 ($p = 0.001$) (Fig. 1b). Furthermore, this difference in HCEnCs yield within the two culture conditions increased gradually at the first passages and then more rapidly at each following passage starting from P2–P3 (Fig. 1c). As such, an insufficient number of HCEnCs were obtained from Dual media for carrying on cell expansion after P4. The cell circularity measurements from P1 to P4 (Fig. 1d) confirmed the morphology observed in Fig. 1a: HCEnCs grown in Single medium were more elongated than their counterparts cultured in Dual media from P2 ($p = 0.01$) to P4 ($p = 0.04$). However, HCEnCs grown in Dual media at high passages (P3 and P4) were found to be larger ($p = 0.03$ and $p = 0.04$, respectively) than their counterparts cultured in Single medium (Fig. 1e), in accordance with the low yield obtained in Dual Media (Fig. 1c).

3.3. Characterization of HCEnCs propagated in Single Medium and Dual Media at mRNA level

To get novel insights into the effect of the two cell culture media on HCEnCs expression, nine genes were analysed using quantitative Real-time PCR in three separate sets of HCEnCs at low (P1) and higher (P4) passages grown in Single medium or Dual media (n = 3) (Table 1, serial numbers 02 to 04) (Fig. 2).

HCEnCs expanded in Dual media expressed higher level of SLC4A11 and COL8A1 at both low (P1, respectively $p = 0.022$ and $p = 0.002$) and high passages (P4, respectively $p = 0.027$ and $p = 0.002$) if compared to Single medium (Fig. 2b–d). Conversely, HCEnCs expanded in Single medium expressed higher levels of ATP1A1 at low passage (P1, $p = 0.019$) when compared to their counterparts propagated in Single medium and comparable levels at high passage (P4, $p = 0.489$) (Fig. 2c). While ATP1A1 remained invariant during passages, the other CE-associated markers CD166 and SLC4A11 decreased in both culture media conditions from P1 to P4. Differently, COL8A1 increased during passages only in HCEnCs expanded in Dual media condition ($p = 0.001$). The EnMT associated marker genes α-SMA (Fig. 2e) and CD44 (Fig. 2f) showed an increase during passages in both conditions while no differences were observed between Single and Dual Media. Intriguingly, COL1A1, an important mediator of tissue wound healing (Mathew-Steiner et al., 2021), resulted upregulated in HCEnCs expanded in Single medium at both low ($p = 0.013$) and high ($p = 0.001$) passages when compared to their respective counterparts propagated in Dual media (Fig. 2g). Moreover, COL1A1 expression remained at negligible levels in HCEnCs expanded in Dual media over passages, whereas significantly increased ($p < 0.001$) from P1 to P4 in HCEnCs expanded in Single medium. Finally, the cell-senescence marker gene CDKN2A (Fig. 2h) showed no statistically significant differences between the two media at both low and high passages and during prolonged culture remained invariable in Single medium but increased in the Dual media condition ($p = 0.011$).

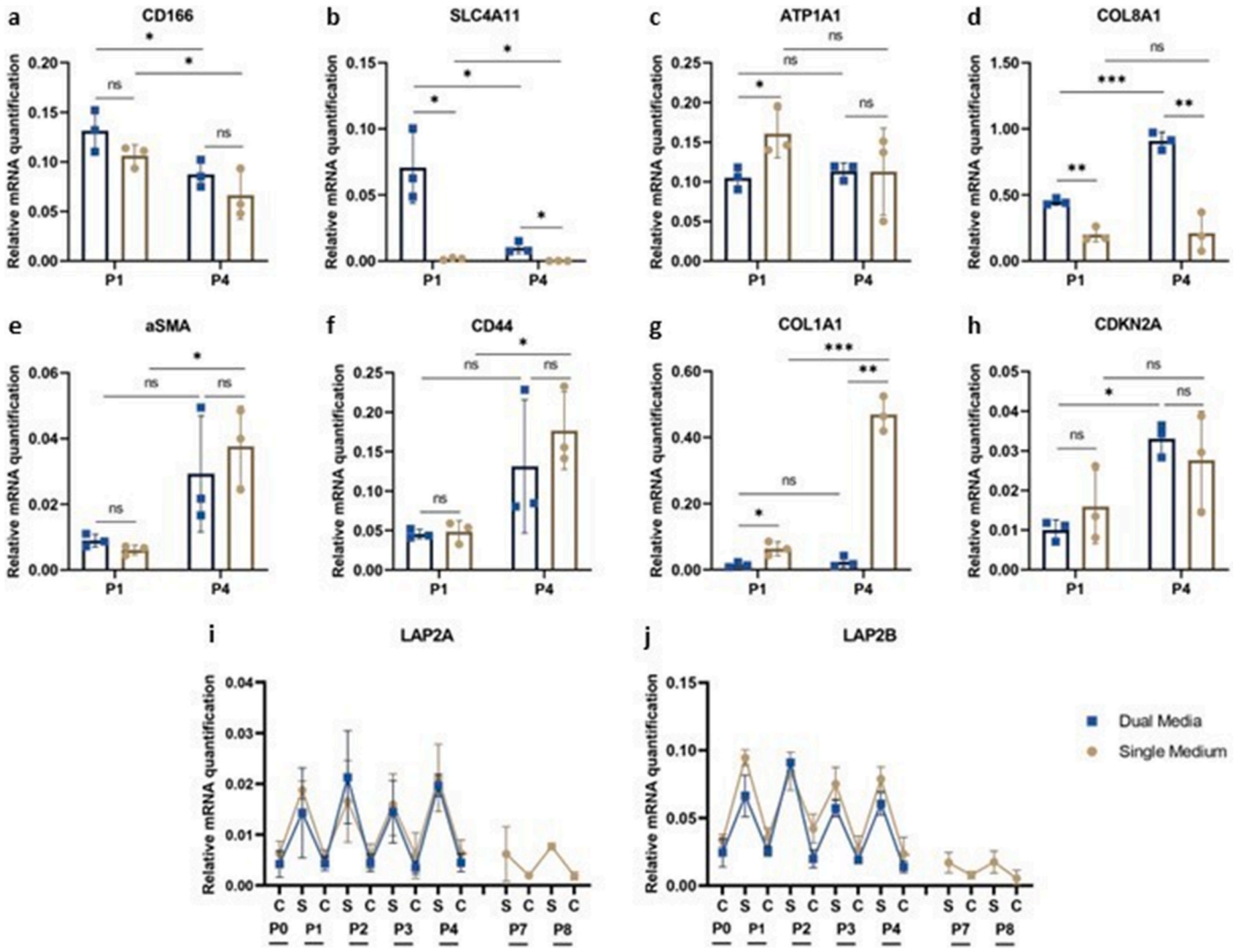

Fig. 2. Gene expression in HCEnCs in Single Medium and Dual Media. Panel of genes, a) CD166, b) SLC4A11, c) ATP1A1, d) COL8A1A, e) α-SMA, f) CD44, g) COL1A1, h) CDKN2A, whose mRNA expression has been evaluated on primary HCEnCs at low (P1) and high (P4) passages in Single Medium and Dual Media by quantitative (q) RT-PCR. i) LAP2A and j) LAP2B gene expression evaluated in HCEnCs cultured in Dual Media and Single medium on primary HCEnCs at all cell passages *in vitro* by qRT-PCR. mRNA levels for each gene are shown as relative expression ± SD (n = 3). Statistical significance was assessed using a Student t-test and set at $p < 0.05$. p values are indicated as following: ns (not significative) when $p > 0.05$, * when $p < 0.05$, ** when $p < 0.01$, *** when $p < 0.001$.

Lastly, LAP2α and LAP2β mRNA expression was evaluated for each subsequent passage, either when HCEnCs were sub-confluent (S, 50 % confluency) or confluent (C, 100 % confluency) in Dual media (Fig. 2i) and Single medium (Fig. 2j). In each passage, HCEnCs exhibited an increased expression of both LAP2α and LAP2β in S condition, when compared to the C cultures both in Single and Dual media, with no significant differences between the two conditions. Moreover, since an insufficient number of HCEnCs were obtained from Dual media for cell expansion beyond P4, HCEnCs were expanded up to P8 only in Single medium. Results demonstrated that LAP2α and β expression levels drastically dropped at high passages to a value close to zero (P7 and P8) and with no difference in LAP2 expression between S and C cultures at high passages ($p > 0.05$).

3.4. *Characterization of HCEnCs propagated in Single Medium and Dual Media at protein level*

Immunofluorescence analysis was carried out on multiple sets of HCEnCs (Table 1) to evaluate differences in protein expression between Single medium and Dual media. Polygonal morphology and CE-associated markers were maintained at low passages in HCEnCs propagated in both conditions, as shown by the expression of pankeratin, cytokeratin (CK)-8 and CK-18, of functional markers such as Na^+K^+/ATPase or tight junction markers as ZO-1 and N-Cadherin (Supplementary, Fig. 2). However, as shown in Fig. 3a, at high passages (P4) HCEnCs displayed an increased α-SMA expression level both in Single medium and Dual media. The quantification of α-SMA^+ cells highlighted that primary HCEnCs expanded in both culture media lost their unique hexagonal/polygonal morphology and acquired a mesenchymal phenotype (Fig. 3b). However, the greater degree of EnMT process was observed in HCEnCs expanded in Single medium, as outlined by higher levels of α-SMA^+ HCEnCs at P4 (Single medium = 32.75 % and Dual media = 18.72 %), in agreement with the phase contrast images and the measurement of cell circularity shown in Fig. 1.

LAP2 expression was further evaluated at protein level by immunocytochemistry, together with expression of the Ki67 proliferation marker (Fig. 3c). Quantification of immunofluorescence analysis on HCEnCs allowed observing that LAP2 protein expression decreased significantly at C in both Single medium and Dual media (p-value respectively <0.05 and < 0.01), if compared with the same cells at the same passage but at S (Fig. 3d). This LAP2 protein modulation between S and C reflected the changes at mRNA level as previously measured

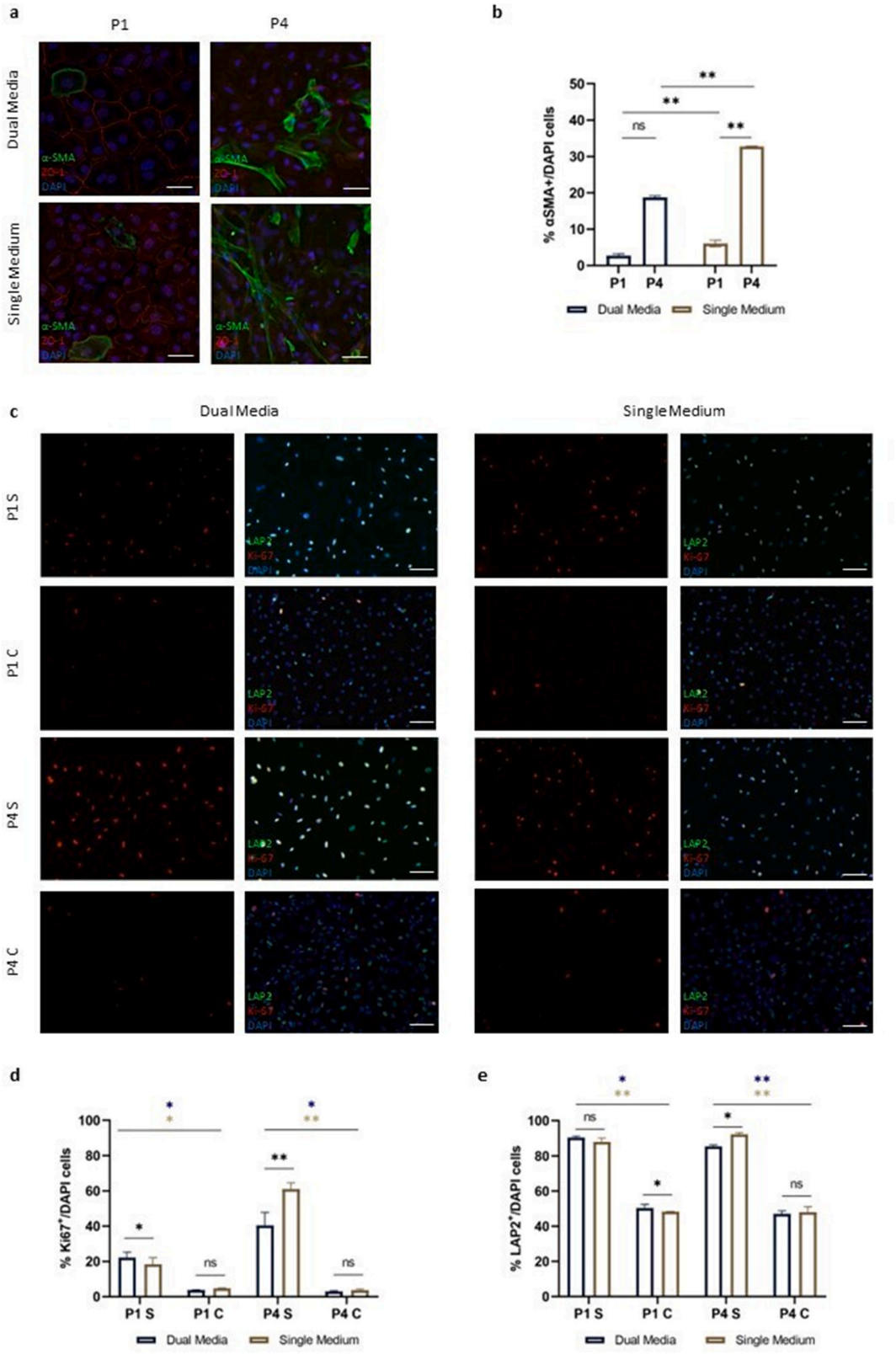

Fig. 3. Protein expression of HCEnCs in Single Medium and Dual media. a) Representative immunofluorescence microscopy images of HCEnCs at P1 and P4, showing expression of α-SMA (green) and ZO-1 (red). DAPI (blue) counterstains nuclei. Scale bar 50 μm. b) Quantification of the percentage of HCEnCs expressing α-SMA protein (±SD) at low (P1) and high (P4) passages, as seen in Fig. 3a. Statistical significance was assessed using a Student t-test (Ratio paired) and set at $p < 0.05$. p-values are indicated as following: ns (not significative) when $p > 0.05$, * when $p < 0.05$, ** when $p < 0.01$, *** when $p < 0.001$ ($n = 3$). c) Representative images of ki67 (red) and LAP2 (green) immunofluorescence staining of HCEnCs at P1 and P4 both at subconfluence (S) and confluence (C). DAPI (blue) counterstained nuclei. Scale bar 20 μm. d) Ki67 and e) LAP2 quantification of immunofluorescence staining as shown in (c) ($n = 3$). Data are presented as mean ± SD. Statistical significance was assessed using a Student t-test and set at $p < 0.05$. p values are indicated as following: ns (not significative) when $p > 0.05$, * when $p < 0.05$, ** when $p < 0.01$. (For interpretation of the references to colour in this figure legend, the reader is referred to the Web version of this article.)

(Fig. 2i and j). In parallel, ki67 expression analysis confirmed that the HCEnCs were actively proliferating at S, when the cells showed a significantly higher LAP2 expression if compared with the C counterpart (Fig. 3e).

3.5. Effect of Y-27632 on HCEnCs derived from old donor corneas cultured in Single Medium

Three pairs of old donor corneas (Table 1, serial numbers 13 to 15) were used to compare HCEnCs cultured in Single Medium with (w/) or without (w/o) 10 μM of Y-27632 (Fig. 4). Representative phase contrast micrographs showed no significant morphological differences in HCEnCs grown in Single medium w/or w/o Y-27632 at both low (P1) and high (P4) passages (Fig. 4a), as well as no significant differences were observed in cell circularity (Fig. 4b) and cell area (Fig. 4c). HCEnCs were counted upon confluency at P1 and P4 (Fig. 4d): the number of HCEnCs grown in Single medium w/o Y-27632 was constantly comparable to their counterpart w/Y-27632 at each analysed passage ($p > 0.05$). Identification of cell cycle phases using flow cytometry showed that at 60 % confluence, both cell populations were distributed among different phases of the cell cycle: 32.1 % and 34 % of the population cultured w/and w/o Y-27632, respectively, was in G2/M phases, in agreement with the cell yields (Fig. 4e).

Seven genes were analysed at mRNA level using quantitative Real-time PCR in three separate sets of HCEnCs at low (P1) and high (P4) passages (Fig. 4g). Intriguingly, all selected genes showed no statistically significant differences ($p > 0.05$) between the two media at both low and high passages. Similarly, at protein level, α-SMA expression was not different in HCEnCs treated with 10 μM of Y-27632, if compared with the untreated control (Fig. 2f).

4. Discussion

The isolation and culture of primary HCEnCs have been described in many reports (Engelmann and Friedl, 1989; Joyce et al., 1989; Ong and Ang, 2021; Parekh et al., 2015; Peh et al., 2011a; Wongvisavavit et al., 2021), even though the results obtained to date on cell growth have been variable. In particular, no protocols specifically designed for clinical application of HCEnCs derived from old donor corneas has been established so far, since expanding these cells results far more challenging (Miyata et al., 2001; Parekh et al., 2017; Wongvisavavit et al., 2021; Zhu and Joyce, 2004). In response to a mitogenic stimulation, HCEnCs from old donors are capable of both entering and completing the cell cycle but respond more slowly and to a lesser extent than cells from young donors (Senoo and Joyce, 2000; Zhu and Joyce, 2004). The low proliferative capacity of HCEnCs derived from old donors is associated to a shorter life span in culture and to a cell size heterogeneity (Enomoto et al., 2006; Joyce and Zhu, 2004; Miyata et al., 2001; Zhu and Joyce, 2004), together with a reduced pump function (O'Neal and Polse, 1986), an altered expression of proteins involved in cell metabolism, protein folding, and protection against oxidative stress (Zhu et al., 2008), as well as truncated telomeres and damaged DNA (Joyce, 2012; Joyce et al., 2011). All these features persuaded researchers to use HCEnCs from young donors to obtain *in vitro* culture that would better resemble an optimal and functional CE (Wongvisavavit et al., 2021). However, the majority of patients requiring treatment for endothelial dysfunction are of elderly age and there are more corneas available for research purposes from old donors, since they are not suitable for transplantation. For this reason, it becomes relevant to investigate effects of different culture media on the growth and morphology of old derived HCEnCs.

Importantly, the present study compares cells isolated from a single donor, which were equally divided between the selected media in order to reduce biases associated with inter-donor variability.

Our results demonstrated that both Single Medium and Dual Media (Kinoshita et al., 2018; Peh et al., 2015b) sustain the culture of HCEnCs derived from old donors, without showing significant morphological (Fig. 1a–d, e) and protein expression (Supplementary Fig. 2) differences at low passages (P1–P2). At P4, HCEnCs cultured in Dual Media appeared more polygonal/hexagonal than their counterpart grown in Single Medium, in line with a higher circularity (Fig. 1a–d). On the other hand, HCEnCs grown in Dual media were found to be larger than those cultured in Single Medium (Fig. 1e), feature that hampered the progression of the culture in Dual Media beyond P4. The increase in cell size is generally related to a senescence-associated proliferation arrest (Lanz et al., 2022; Schmitt et al., 2022), consistently with a lower HCEnCs yield found at harvesting (Fig. 1b and c) and with the up-regulation of cell senescence-associated marker CDKN2A (Fig. 2h)(Hernandez-Segura et al., 2018).

Analysis of gene expression suggested that the Dual Media better preserve a corneal endothelial phenotype, showing a higher SLC4A11 expression than the Single Media at both low and high passages *in vitro* (Fig. 2b). Similarly, COL8A1 expression, secreted by HCEnCs as a component of the Descemet's membrane (Chen et al., 2001), was higher in Dual Media than Single Medium (Fig. 2d). Descemet's membrane is composed by a precise pattern of hexagonal collagen structures that serve as a supportive scaffold for HCEnCs (Walckling et al., 2020). Since COL8 is an essential component of this pattern, an elevated expression of this marker found in Dual Media might reflect the maintenance of hexagonal shape in this culture condition. On the other hand, ATP1A1, an important functional marker used to detect CE pump function, presented a higher expression in HCEnCs grown in Single Medium at low passages (Fig. 2c). Fibroblastic markers associated with the EnMT, namely α-SMA (He et al., 2016) or CD44 (Okumura et al., 2014a), showed a similar expression profile in the two media (Fig. 2e and f). Importantly, CD44 plays a critical role as a major adhesion molecule of the ECM and in TGF-β–mediated mesenchymal phenotype induction, and loss of CD44 reportedly arrests those changes (Nagano and Saya, 2004). Absence of CD44 has been considered the hallmark of high quality cultured HCEnCs (Frausto et al., 2020), associated with a mature phenotype (Frausto et al., 2020; Ueno et al., 2016). A subpopulation of cultured HCEnCs found with high positivity for CD44 expression marker has been associated with anaerobic glycolysis and cell-state transition, differently from the CD44 negative subpopulation that presented disposition for mitochondria-dependent oxidative phosphorylation (Hamuro et al., 2016a). Moreover, the latter subpopulation was found with less secreted pyruvic and lactic acid in the culture supernatants than CD44 positive subpopulation, suggesting a possible metabolic rewiring and cell state transition between the two subpopulation (Hamuro et al., 2020). COL1A1, a marker associated to tissue wound healing (Mathew-Steiner et al., 2021), was more expressed in cells grown in Single Medium than in Dual media (Fig. 2g). These data are consistent with Mehta's results (Peh et al., 2015b) in which HCEnCs cultured with the Dual media approach expressed higher levels of SLC4A11, and COL8A1, whereas those grown in proliferation medium alone showed higher levels of COL1A1. An immediate visualization and comparison of gene expression between the two conditions is shown in a representative HeatMap (Fig. 5b).

Protein expression of α-SMA at P4 increased in both conditions, even though with a larger extent in Single medium than Dual Media (Fig. 3a and b). These results reflect the elongated morphology (Fig. 1) and correlate with an elevated proliferation rate at P4 (Fig. 3c and d) observed in Single medium, a direct consequence of a higher mitogenic stimulation if compared to the Dual media (Fig. 5c). LAP2, as previously described by our research group (Maurizi and Merra, 2022), confirmed its up-regulation in sub-confluent cultures both in Single Medium and Dual Media at P1 and P4 (Fig. 2i and j). Moreover, as the passages increase further and the cells become more fibroblastic (P7–P8 in Single Medium), the LAP2 expression drastically decreased (Fig. 2i and j), confirming how LAP2 regulation correlates with the quality of HCEnCs culture, as previously observed (Maurizi and Merra, 2022). The data obtained at high passages for LAP2 need further confirmation in a larger cohort of HCEnCs, as human donors are highly heterogeneous.

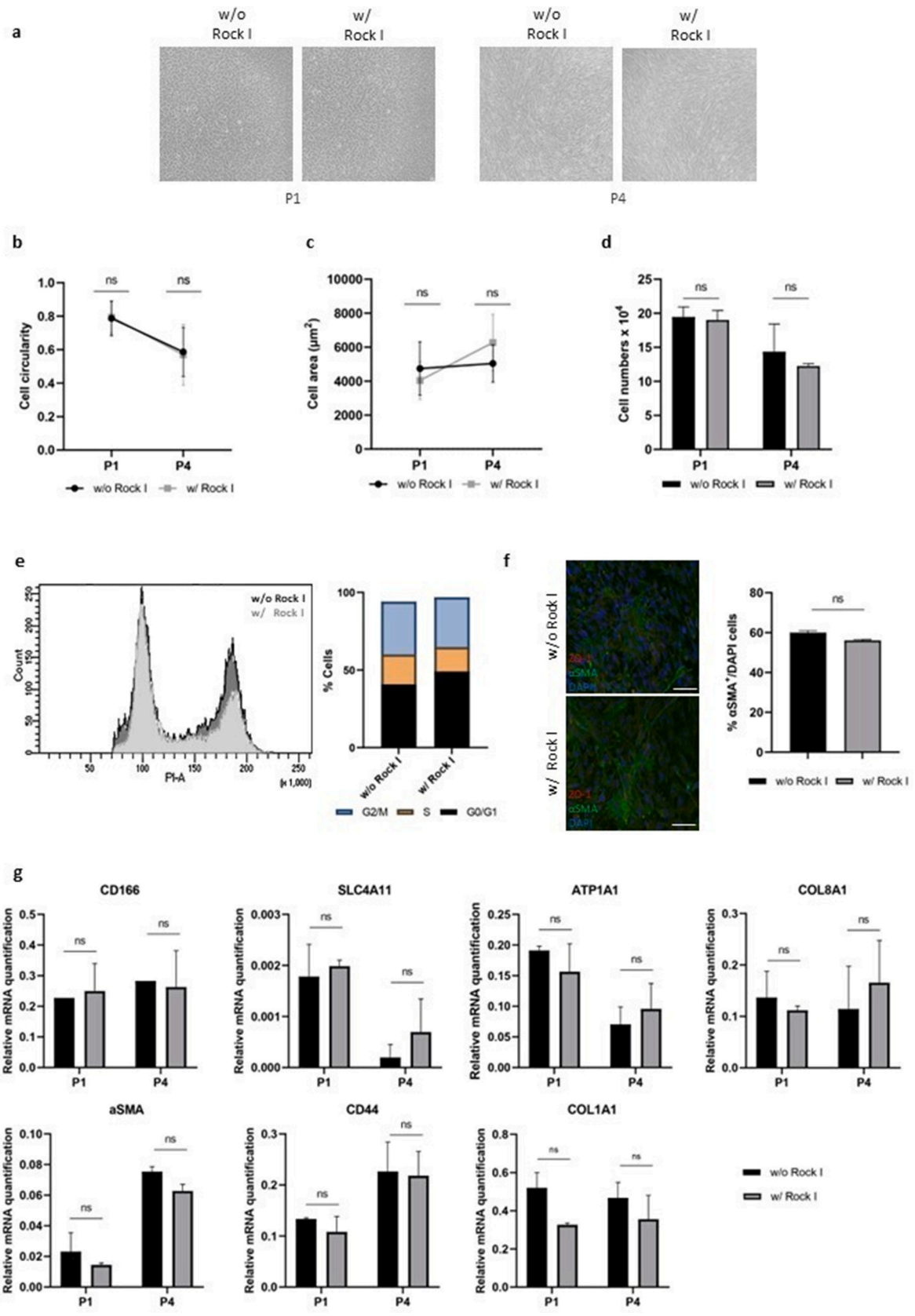

(caption on next page)

Fig. 4. Comparison of HCEnCs in Single Medium w/and w/o Rock Inhibitor. a) Representative sets of phase–contrast photomicrographs showing morphology of HCEnCs at P1 and P4 (n = 3). b) Cell circularity of HCEnCs at P1 and P4 at confluence. Cell circularity is expressed as values ± SD (n = 3). c) Cell size of HCEnCs at P1 and P4 at confluence. Quantitative data are expressed as values ± SD (n = 3). d) HCEnCs yield at harvesting at P1 and P4 (n = 3). Total cell numbers are expressed as values ± SD. e) Cells distribution in the cell cycle phases identified by Propidium Iodide flow cytofluorometric analysis and plotted in a representative graph for each condition on the left. The cell cycle phases were assessed when HCEnCs were at 60 % confluence (subconfluence, sub). The panel on the right represents a bar chart of the flow cytofluorometric analysis shown on the left comparing HCEnCs at P5 in Single Medium w/and w/o Rock Inhibitor. Experiments were performed n = 2. Results are presented as mean ± SD. f) Representative immunofluorescence microscopy images of HCEnCs at P5, showing the expression of α-SMA (green) and ZO-1 (red). DAPI (blue) counterstains nuclei. Scale bar 20 μm. Quantification of the percentage of HCEnCs expressing α-SMA protein (±SD), as seen shown on the left (n = 3). g) Panel of genes (CD166, SLC4A11, ATP1A1, COL8A1A, α-SMA, CD44, COL1A1) whose mRNA expression has been evaluated on primary HCEnCs at P1 and P4 by qRT-PCR. Statistical significance was assessed using a Student t-test and set at $p < 0.05$. p-values are indicated as following: ns (not significative) when $p > 0.05$, * when $p < 0.05$, ** when $p < 0.01$, *** when $p < 0.001$. (For interpretation of the references to colour in this figure legend, the reader is referred to the Web version of this article.)

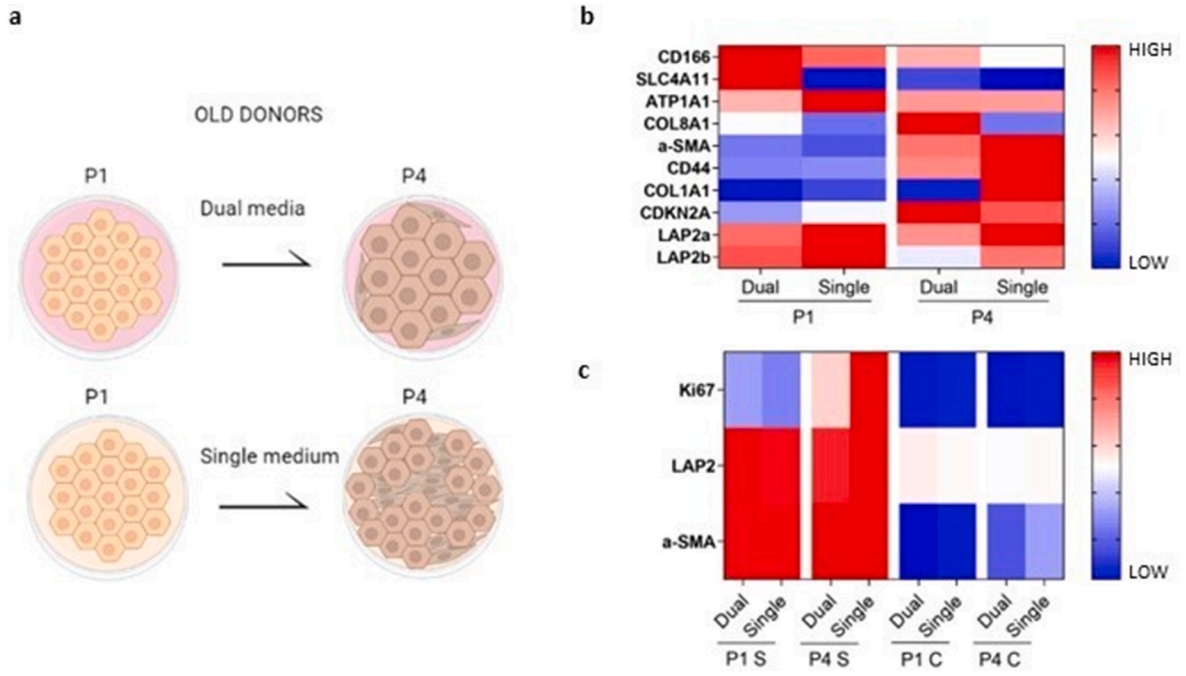

Fig. 5. Schematic representation of results obtained in this study. a) Schematic representation of the morphology of HCEnCs derived from old donors cultured for several passages *in vitro* in Dual Media and Single Medium. Image created with Biorender.com. b) Heatmap illustrating the differentially expressed genes in Dual Media and Single Medium at P1 and P4 *in vitro*. c) Heatmap illustrating the differentially expressed proteins in Dual Media and Single Medium at P1 and P4 in sub-confluent and confluent state *in vitro*. Heatmap scale colours represent expression values that have been normalised within each gene/protein. (For interpretation of the references to colour in this figure legend, the reader is referred to the Web version of this article.)

The effects of Y-27632 on HCEnCs derived from old donor corneas were studied since ROCK inhibitor has been previously reported to inhibit apoptosis and increase cellular adhesion and proliferation of both primate and human CEnCs (Okumura et al., 2009, 2014b). We did not find any difference between the Single Medium with/without Y-27632 on cell adhesion, proliferation and CE-associated markers expression (Fig. 4). A similar observation was previously reported by Mehta and colleagues in Dual media (Peh et al., 2015a) and by Pipparelli and colleagues, showing that Y-27632 had no effect on the proliferative capacity of HCEnCs from donors aged 73 ± 3 years (Pipparelli et al., 2013). Thus, the use of Y-27632 in Single medium may be appropriate exclusively for cultures of HCEnCs established from young donors (Bartakova et al., 2018).

Overall, our results showed that the Dual Media maintained more efficiently the hexagonal phenotype but increased cell size of old donor derived HCEnCs *in vitro*, while the Single Medium allowed a higher proliferation rate and a longer term culture at the expense of morphology maintenance (Fig. 5a). Similar studies on HCEnCs from young donors (age <40 years) proposed the Dual Media as a valid alternative to Single Medium, providing evidences of maintaining a polygonal morphology, expression of critical markers and cell functions for several passages (Bartakova et al., 2018; Frausto et al., 2020; Peh et al., 2011b). In particular, low-mitogenic media allow HCEnCs to recover hexagonal morphology, preserve cell function over multiple passages (as measured by higher trans-endothelial electrical resistance) while obtaining an increased cell yield (Bartakova et al., 2018), maintain a robust HCEnCs-specific gene expression profile and functional barrier as well as pump activity (Frausto et al., 2020). In this study, we have shown that, for old donor derived HCEnCs, either Single medium or Dual Media preserve the typical CE features at low passages, while maintaining cell morphology and functional phenotype at high passages remains a challenge.

Additional measures that could improve the success rate of HCEnCs cultures from old donor corneas need to be taken into consideration in the next future. Based on the CE metabolic recovery observed upon organ culture of old donors (mean age 62–65 years) (Redbrake et al., 1999), an initial step of DM–CE sheet stabilization was introduced overnight (Zhu and Joyce, 2004) or for several days in growth factor-depleted culture medium prior to cell isolation, showing increase in viable HCEnCs deriving from donors (mean age of 69 years) (Spinozzi et al., 2018). Indeed, the removal of apoptotic cells prior to cell isolation is beneficial as apoptotic factors released into the media negatively impact their viable neighbours (Gregory and Pound, 2010). In addition, accelerating adhesion of HCEnCs with the assistance of a viscoelastic

solution has shown an increased proliferation rate for HCEnCs isolated from old donors (Parekh et al., 2019a), the same effect obtained by reducing the incubator partial pressure of oxygen to the physiological value of approximately 21 mmHg (~2.8 %) (Carreau et al., 2011), due to reduced oxidative stress (Patel et al., 2022; Sheerin et al., 2012).

The described precautions could be introduced to compare culture media in order to introduce more parameters and define an optimised protocol for old derived HCEnCs.

5. Conclusion

A culture media capable to ameliorate preservation of old donor derived HCEnCs, more frequently available from eye banks, could have a broad impact for HCEnCs based therapies. This work revealed novel aspects of HCEnCs derived from old donors when cultured with different media and leads the path for further investigations towards using these cells for clinical applications in order to reach a larger cohort of patients.

Funding

This research did not receive any specific grant from funding agencies in the public or not-for-profit sectors. Part of the funding comes from Holostem Terapie Avanzate.

CRediT authorship contribution statement

Alessia Merra: Conceptualization, Data curation, Formal analysis, Investigation, Writing – original draft, Writing – review & editing. **Eleonora Maurizi:** Conceptualization, Formal analysis, Investigation, Methodology, Supervision, Writing – original draft, Writing – review & editing. **Graziella Pellegrini:** Funding acquisition, Resources, Supervision, Writing – review & editing.

Declaration of competing interest

We declare that we have no financial or personal relationships with other people or organizations that could inappropriately influence our work, and there is no professional or other personal interest of any nature or kind in any product, service and/or company that could be construed as influencing the position presented in, or the review of, the manuscript entitled.

Data availability

Data will be made available on request.

Acknowledgements

The authors would like to thank Prof. Macaluso, Dr. Chiappini, Dr. Schiroli and Dr. Adamo for their contribution and, in particular, the people who donated their organs for research and medical purposes.

Appendix A. Supplementary data

Supplementary data to this article can be found online at https://doi.org/10.1016/j.exer.2024.109815.

References

Bartakova, A., Kuzmenko, O., Alvarez-Delfin, K., Kunzevitzky, N.J., Goldberg, J.L., 2018. A cell culture approach to optimized human corneal endothelial cell function. Invest. Ophthalmol. Vis. Sci. 59, 1617–1629.
Baum, J.L., Niedra, R., Davis, C., Yue, B.Y., 1979. Mass culture of human corneal endothelial cells. Arch. Ophthalmol. 97, 1136–1140.
Beaulieu Leclerc, V., Roy, O., Santerre, K., Proulx, S., 2018. TGF-β1 promotes cell barrier function upon maturation of corneal endothelial cells. Sci. Rep. 8, 4438.
Carreau, A., El Hafny-Rahbi, B., Matejuk, A., Grillon, C., Kieda, C., 2011. Why is the partial oxygen pressure of human tissues a crucial parameter? Small molecules and hypoxia. J. Cell Mol. Med. 15, 1239–1253.
Català, P., Thuret, G., Skottman, H., Mehta, J.S., Parekh, M., S, N.D., Collin, R.W.J., Nuijts, R., Ferrari, S., LaPointe, V.L.S., Dickman, M.M., 2022. Approaches for corneal endothelium regenerative medicine. Prog. Retin. Eye Res. 87, 100987.
Chen, K.H., Azar, D., Joyce, N.C., 2001. Transplantation of adult human corneal endothelium ex vivo: a morphologic study. Cornea 20, 731–737.
Chng, Z., Peh, G.S., Herath, W.B., Cheng, T.Y., Ang, H.P., Toh, K.P., Robson, P., Mehta, J. S., Colman, A., 2013. High throughput gene expression analysis identifies reliable expression markers of human corneal endothelial cells. PLoS One 8, e67546.
Choi, J.S., Kim, E.Y., Kim, M.J., Khan, F.A., Giegengack, M., D'Agostino Jr., R., Criswell, T., Khang, G., Soker, S., 2014. Factors affecting successful isolation of human corneal endothelial cells for clinical use. Cell Transplant. 23, 845–854.
Cullen, A.P., 2002. Photokeratitis and other phototoxic effects on the cornea and conjunctiva. Int. J. Toxicol. 21, 455–464.
Davies, E., Jurkunas, U., Pineda 2nd, R., 2021. Pilot study of corneal clearance with the use of a rho-kinase inhibitor after descemetorhexis without endothelial keratoplasty for fuchs endothelial corneal dystrophy. Cornea 40, 899–902.
De Luca, M., D'Anna, F., Bondanza, S., Franzi, A.T., Cancedda, R., 1988. Human epithelial cells induce human melanocyte growth in vitro but only skin keratinocytes regulate its proper differentiation in the absence of dermis. J. Cell Biol. 107, 1919–1926.
Engelmann, K., Böhnke, M., Friedl, P., 1988. Isolation and long-term cultivation of human corneal endothelial cells. Invest. Ophthalmol. Vis. Sci. 29, 1656–1662.
Engelmann, K., Friedl, P., 1989. Optimization of culture conditions for human corneal endothelial cells. In Vitro Cell. Dev. Biol. 25, 1065–1072.
Enomoto, K., Mimura, T., Harris, D.L., Joyce, N.C., 2006. Age differences in cyclin-dependent kinase inhibitor expression and rb hyperphosphorylation in human corneal endothelial cells. Invest. Ophthalmol. Vis. Sci. 47, 4330–4340.
Frausto, R.F., Swamy, V.S., Peh, G.S.L., Boere, P.M., Hanser, E.M., Chung, D.D., George, B.L., Morselli, M., Kao, L., Azimov, R., Wu, J., Pellegrini, M., Kurtz, I., Mehta, J.S., Aldave, A.J., 2020. Phenotypic and functional characterization of corneal endothelial cells during in vitro expansion. Sci. Rep. 10, 7402.
Gain, P., Jullienne, R., He, Z., Aldossary, M., Acquart, S., Cognasse, F., Thuret, G., 2016. Global survey of corneal transplantation and eye banking. JAMA Ophthalmol. 134, 167–173.
Galvis, V., Berrospi, R.D., Arias, J.D., Tello, A., 2017. Heads up Descemet Membrane Endothelial Keratoplasty Performed Using a 3D Visualization System, 2017:rjx231.
Galvis, V., Tello, A., Gutierrez Á, J., 2013. Human corneal endothelium regeneration: effect of ROCK inhibitor. Invest. Ophthalmol. Vis. Sci. 54, 4971–4973.
Gregory, C.D., Pound, J.D., 2010. Microenvironmental influences of apoptosis in vivo and in vitro. Apoptosis : Int. J. Programmed Cell Death 15, 1029–1049.
Hamuro, J., Numa, K., Fujita, T., Toda, M., Ueda, K., Tokuda, Y., Mukai, A., Nakano, M., Ueno, M., Kinoshita, S., Sotozono, C., 2020. Metabolites interrogation in cell fate decision of cultured human corneal endothelial cells. Invest. Ophthalmol. Vis. Sci. 61, 10.
Hamuro, J., Ueno, M., Asada, K., Toda, M., Montoya, M., Sotozono, C., Kinoshita, S., 2016a. Metabolic plasticity in cell state homeostasis and differentiation of cultured human corneal endothelial cells. Invest. Ophthalmol. Vis. Sci. 57, 4452–4463.
Hamuro, J., Ueno, M., Toda, M., Sotozono, C., Montoya, M., Kinoshita, S., 2016b. Cultured human corneal endothelial cell aneuploidy dependence on the presence of heterogeneous subpopulations with distinct differentiation phenotypes. Invest. Ophthalmol. Vis. Sci. 57, 4385–4392.
He, J., Kakazu, A.H., Bazan, N.G., Bazan, H.E., 2011. Aspirin-triggered lipoxin A4 (15-epi-LXA4) increases the endothelial viability of human corneas storage in Optisol-GS. J. Ocul. Pharmacol. Therapeut. : Offic. J. Assoc. Ocular Pharmacol. Therapeut. 27, 235–241.
He, Z., Forest, F., Gain, P., Rageade, D., Bernard, A., Acquart, S., Peoc'h, M., Defoe, D.M., Thuret, G., 2016. 3D map of the human corneal endothelial cell. Sci. Rep. 6, 29047.
Hemaya, M., Hemaya, M., Habeeb, A., 2023. Evaluating keratoplasty for fuchs' endothelial corneal dystrophy: a literature review. Cureus 15, e33639.
Hernandez-Segura, A., Nehme, J., Demaria, M., 2018. Hallmarks of cellular senescence. Trends Cell Biol. 28, 436–453.
Ishino, Y., Sano, Y., Nakamura, T., Connon, C.J., Rigby, H., Fullwood, N.J., Kinoshita, S., 2004. Amniotic membrane as a carrier for cultivated human corneal endothelial cell transplantation. Invest. Ophthalmol. Vis. Sci. 45, 800–806.
Jäckel, T., Knels, L., Valtink, M., Funk, R.H., Engelmann, K., 2011. Serum-free corneal organ culture medium (SFM) but not conventional minimal essential organ culture medium (MEM) protects human corneal endothelial cells from apoptotic and necrotic cell death. Br. J. Ophthalmol. 95, 123–130.
Joyce, N.C., 2003. Proliferative capacity of the corneal endothelium. Prog. Retin. Eye Res. 22, 359–389.
Joyce, N.C., 2012. Proliferative capacity of corneal endothelial cells. Exp. Eye Res. 95, 16–23.
Joyce, N.C., Harris, D.L., Zhu, C.C., 2011. Age-related gene response of human corneal endothelium to oxidative stress and DNA damage. Invest. Ophthalmol. Vis. Sci. 52, 1641–1649.
Joyce, N.C., Matkin, E.D., Neufeld, A.H., 1989. Corneal endothelial wound closure in vitro. Effects of EGF and/or indomethacin. Invest. Ophthalmol. Vis. Sci. 30, 1548–1559.
Joyce, N.C., Zhu, C.C., 2004. Human corneal endothelial cell proliferation: potential for use in regenerative medicine. Cornea 23, S8–s19.
Joyce, N.C., Zhu, C.C., Harris, D.L., 2009. Relationship among oxidative stress, DNA damage, and proliferative capacity in human corneal endothelium. Invest. Ophthalmol. Vis. Sci. 50, 2116–2122.

Kinoshita, S., Koizumi, N., Ueno, M., Okumura, N., Imai, K., Tanaka, H., Yamamoto, Y., Nakamura, T., Inatomi, T., Bush, J., Toda, M., Hagiya, M., Yokota, I., Teramukai, S., Sotozono, C., Hamuro, J., 2018. Injection of cultured cells with a ROCK inhibitor for bullous keratopathy. N. Engl. J. Med. 378, 995–1003.
Konomi, K., Zhu, C., Harris, D., Joyce, N.C., 2005. Comparison of the proliferative capacity of human corneal endothelial cells from the central and peripheral areas. Invest. Ophthalmol. Vis. Sci. 46, 4086–4091.
Krohn, J., Høvding, G., 2005. The influence of donor age and cause of death on corneal endothelial cell density. Acta Ophthalmol. Scand. 83, 746–750.
Lamouille, S., Xu, J., Derynck, R., 2014. Molecular mechanisms of epithelial-mesenchymal transition. Nat. Rev. Mol. Cell Biol. 15, 178–196.
Lanz, M.C., Zatulovskiy, E., Swaffer, M.P., Zhang, L., Ilerten, I., Zhang, S., You, D.S., Marinov, G., McAlpine, P., Elias, J.E., Skotheim, J.M., 2022. Increasing cell size remodels the proteome and promotes senescence. Mol. Cell 82, 3255–3269 e3258.
Lass, J.H., Benetz, B.A., Patel, S.V., Szczotka-Flynn, L.B., O'Brien, R., Ayala, A.R., Maguire, M.G., Daoud, Y.J., Greiner, M.A., Hannush, S.B., Lee, W.B., Mauger, T.F., Menegay, H.J., Mifflin, M.D., Raizman, M.B., Rose-Nussbaumer, J., Schultze, R.L., Schmidt, G.A., Sugar, A., Terry, M.A., Verdier, D.D., 2019. Donor, recipient, and operative factors associated with increased endothelial cell loss in the cornea preservation time study. JAMA Ophthalmol. 137, 185–193.
Lee, J.G., Ko, M.K., Kay, E.P., 2012. Endothelial mesenchymal transformation mediated by IL-1β-induced FGF-2 in corneal endothelial cells. Exp. Eye Res. 95, 35–39.
Li, C., Dong, F., Jia, Y., Du, H., Dong, N., Xu, Y., Wang, S., Wu, H., Liu, Z., Li, W., 2013. Notch signal regulates corneal endothelial-to-mesenchymal transition. Am. J. Pathol. 183, 786–795.
Li, X., Li, Z., Qiu, L., Zhao, C., Hu, Z., 2005. Nerve growth factor modulate proliferation of cultured rabbit corneal endothelial cells and epithelial cells. J. Huazhong Univ. Sci. Technol. Med. sci. = Hua zhong ke ji da xue xue bao. Yi xue Ying De wen ban = Huazhong keji daxue xuebao. Yixue Yingdewen ban 25, 575–577.
Mathew-Steiner, S.S., Roy, S., Sen, C.K., 2021. Collagen in wound healing. Bioengineering 8, 63.
Maurice, D.M., 1957. The structure and transparency of the cornea. J. Physiol. 136, 263–286.
Maurizi, E., Adamo, D., Magrelli, F.M., Galaverni, G., Attico, E., Merra, A., Maffezzoni, M.B.R., Losi, L., Genna, V.G., Sceberras, V., 2021. Regenerative medicine of epithelia: lessons from the past and future goals. Front. Bioeng. Biotechnol. 9, 652214.
Maurizi, E., Merra, A., 2022. Fluctuations in corneal endothelial LAP2 expression levels correlate with passage dependent declines in their cell proliferative activity, 23.
Maurizi, E., Merra, A., Macaluso, C., Schiroli, D., Pellegrini, G., 2023. GSK-3 inhibition reverts mesenchymal transition in primary human corneal endothelial cells. Eur. J. Cell Biol. 102, 151302.
Maurizi, E., Schiroli, D., Atkinson, S.D., Mairs, L., Courtney, D.G., O'Hagan, B., McGilligan, V.E., Pagnamenta, A.T., Taylor, J.C., Vasquez, J.J., 2019. A novel role for CRIM1 in the corneal response to UV and pterygium development. Exp. Eye Res. 179, 75–92.
Maurizi, E., Schiroli, D., Zini, R., Limongelli, A., Mistò, R., Macaluso, C., Pellegrini, G., 2020. A fine-tuned β-catenin regulation during proliferation of corneal endothelial cells revealed using proteomics analysis. Sci. Rep. 10, 1–16.
Mimura, T., Yamagami, S., Amano, S., 2013. Corneal endothelial regeneration and tissue engineering. Prog. Retin. Eye Res. 35, 1–17.
Mishima, S., 1982. Clinical investigations on the corneal endothelium-XXXVIII Edward Jackson memorial lecture. Am. J. Ophthalmol. 93, 1–29.
Miyata, K., Drake, J., Osakabe, Y., Hosokawa, Y., Hwang, D., Soya, K., Oshika, T., Amano, S., 2001. Effect of donor age on morphologic variation of cultured human corneal endothelial cells. Cornea 20, 59–63.
Musa, M., Zeppieri, M., 2023. An overview of corneal transplantation in the past decade, 13, 264–279.
Nagano, O., Saya, H., 2004. Mechanism and biological significance of CD44 cleavage. Cancer Sci. 95, 930–935.
Nanavaty, M.A., Wang, X., Shortt, A.J., 2014. Endothelial keratoplasty versus penetrating keratoplasty for Fuchs endothelial dystrophy. Cochrane Database Syst. Rev. 2, Cd008420.
Numa, K., Imai, K., Ueno, M., Kitazawa, K., Tanaka, H., Bush, J.D., Teramukai, S., Okumura, N., Koizumi, N., Hamuro, J., Sotozono, C., Kinoshita, S., 2021. Five-year follow-up of first 11 patients undergoing injection of cultured corneal endothelial cells for corneal endothelial failure. Ophthalmology 128, 504–514.
O'Neal, M.R., Polse, K.A., 1986. Decreased endothelial pump function with aging. Invest. Ophthalmol. Vis. Sci. 27, 457–463.
Okumura, N., Hirano, H., Numata, R., Nakahara, M., Ueno, M., Hamuro, J., Kinoshita, S., Koizumi, N., 2014a. Cell surface markers of functional phenotypic corneal endothelial cells. Invest. Ophthalmol. Vis. Sci. 55, 7610–7618.
Okumura, N., Kay, E.P., Nakahara, M., Hamuro, J., Kinoshita, S., Koizumi, N., 2013. Inhibition of TGF-β signaling enables human corneal endothelial cell expansion in vitro for use in regenerative medicine. PLoS One 8, e58000.
Okumura, N., Kinoshita, S., Koizumi, N., 2017. Application of Rho Kinase Inhibitors for the Treatment of Corneal Endothelial Diseases, 2646904, 2017.
Okumura, N., Koizumi, N., Ueno, M., Sakamoto, Y., Takahashi, H., Hamuro, J., Kinoshita, S., 2011a. The new therapeutic concept of using a rho kinase inhibitor for the treatment of corneal endothelial dysfunction. Cornea 30 (Suppl. 1), S54–S59.
Okumura, N., Koizumi, N., Ueno, M., Sakamoto, Y., Takahashi, H., Hirata, K., Torii, R., Hamuro, J., Kinoshita, S., 2011b. Enhancement of corneal endothelium wound healing by Rho-associated kinase (ROCK) inhibitor eye drops. Br. J. Ophthalmol. 95, 1006–1009.
Okumura, N., Nakano, S., Kay, E.P., Numata, R., Ota, A., Sowa, Y., Sakai, T., Ueno, M., Kinoshita, S., Koizumi, N., 2014b. Involvement of cyclin D and p27 in cell proliferation mediated by ROCK inhibitors Y-27632 and Y-39983 during corneal endothelium wound healing. Invest. Ophthalmol. Vis. Sci. 55, 318–329.
Okumura, N., Ueno, M., Koizumi, N., Sakamoto, Y., Hirata, K., Hamuro, J., Kinoshita, S., 2009. Enhancement on primate corneal endothelial cell survival in vitro by a ROCK inhibitor. Invest. Ophthalmol. Vis. Sci. 50, 3680–3687.
Ong, H.S., Ang, M., 2021. Evolution of therapies for the corneal endothelium: past, present and future approaches, 105, 454–467.
Parekh, M., Ahmad, S., Ruzza, A., Ferrari, S., 2017. Human corneal endothelial cell cultivation from old donor corneas with forced attachment. Sci. Rep. 7, 142.
Parekh, M., Ferrari, S., Sheridan, C., Kaye, S., Ahmad, S., 2015. Concise review: an update on the culture of human corneal endothelial cells for transplantation. Stem Cells Translat. Med. 5, 258–264.
Parekh, M., Peh, G., Mehta, J.S., Ramos, T., Ponzin, D., Ahmad, S., Ferrari, S., 2019a. Passaging capability of human corneal endothelial cells derived from old donors with and without accelerating cell attachment. Exp. Eye Res. 189, 107814.
Parekh, M., Romano, V., Ruzza, A., Kaye, S.B., Ponzin, D., Ahmad, S., Ferrari, S., 2019b. Increasing donor endothelial cell pool by culturing cells from discarded pieces of human donor corneas for regenerative treatments. J. Ophthalmol., 2525384, 2019.
Patel, S.P., Calle Gonzalez, B., Paone, N., Mueller, C., Floss, J.C., Sousa, M.E., Shi, M.Y., 2022. Effect of physiological oxygen on primary human corneal endothelial cell cultures. Translat. Vis. Sci. Technol. 11, 33-33.
Peh, G.S., Adnan, K., George, B.L., Ang, H.P., Seah, X.Y., Tan, D.T., Mehta, J.S., 2015a. The effects of Rho-associated kinase inhibitor Y-27632 on primary human corneal endothelial cells propagated using a dual media approach. Sci. Rep. 5, 9167.
Peh, G.S., Beuerman, R.W., Colman, A., Tan, D.T., Mehta, J.S., 2011a. Human corneal endothelial cell expansion for corneal endothelium transplantation: an overview. Transplantation 91, 811–819.
Peh, G.S., Chng, Z., Ang, H.P., Cheng, T.Y., Adnan, K., Seah, X.Y., George, B.L., Toh, K.P., Tan, D.T., Yam, G.H., Colman, A., Mehta, J.S., 2015b. Propagation of human corneal endothelial cells: a novel dual media approach. Cell Transplant. 24, 287–304.
Peh, G.S., Lee, M.X., Wu, F.Y., Toh, K.P., Balehosur, D., Mehta, J.S., 2012. Optimization of human corneal endothelial cells for culture: the removal of corneal stromal fibroblast contamination using magnetic cell separation. Int. J. Biomater., 601302, 2012.
Peh, G.S., Toh, K.P., Wu, F.Y., Tan, D.T., Mehta, J.S., 2011b. Cultivation of human corneal endothelial cells isolated from paired donor corneas. PLoS One 6, e28310.
Pellegrini, G., Golisano, O., Paterna, P., Lambiase, A., Bonini, S., Rama, P., De Luca, M., 1999. Location and clonal analysis of stem cells and their differentiated progeny in the human ocular surface. JCB (J. Cell Biol.) 145, 769–782.
Pipparelli, A., Arsenijevic, Y., Thuret, G., Gain, P., Nicolas, M., Majo, F., 2013. ROCK inhibitor enhances adhesion and wound healing of human corneal endothelial cells. PLoS One 8, e62095.
Redbrake, C., Becker, J., Salla, S., Stollenwerk, R., Reim, M., 1994. The influence of the cause of death and age on human corneal metabolism. Invest. Ophthalmol. Vis. Sci. 35, 3553–3556.
Redbrake, C., Salla, S., Frantz, A., Reim, M., 1999. Metabolic changes of the human donor cornea during organ-culture. Acta Ophthalmol. Scand. 77, 266–272.
Romano, D., Aiello, F., Parekh, M., Levis, H.J., Gadhvi, K.A., Moramarco, A., Viola, P., Fontana, L., Semeraro, F., Romano, V., 2023. Incidence and management of early postoperative complications in lamellar corneal transplantation, 261, 3097–3111.
Roy, O., Beaulieu Leclerc, V., Bourget, J.-M., Thériault, M., Proulx, S., 2015a. Understanding the process of corneal endothelial morphological change in vitro. Invest. Ophthalmol. Vis. Sci. 56, 1228–1237.
Roy, O., Leclerc, V.B., Bourget, J.M., Thériault, M., Proulx, S., 2015b. Understanding the process of corneal endothelial morphological change in vitro. Invest. Ophthalmol. Vis. Sci. 56, 1228–1237.
Schmitt, C.A., Wang, B., Demaria, M., 2022. Senescence and cancer — role and therapeutic opportunities. Nat. Rev. Clin. Oncol. 19, 619–636.
Schneider, C.A., Rasband, W.S., Eliceiri, K.W., 2012. NIH Image to ImageJ: 25 years of image analysis. Nat. Methods 9, 671–675.
Senoo, T., Joyce, N.C., 2000. Cell cycle kinetics in corneal endothelium from old and young donors. Invest. Ophthalmol. Vis. Sci. 41, 660–667.
Shamsuddin, A.K., Nirankari, V.S., Purnell, D.M., Chang, S.H., 1986. Is the corneal posterior cell layer truly endothelial? Ophthalmology 93, 1298–1303.
Sheerin, A.N., Smith, S.K., Jennert-Burston, K., Brook, A.J., Allen, M.C., Ibrahim, B., Jones, D., Wallis, C., Engelmann, K., Rhys-Williams, W., Faragher, R.G., Kipling, D., 2012. Characterization of cellular senescence mechanisms in human corneal endothelial cells. Aging Cell 11, 234–240.
Spinozzi, D., Miron, A., Bruinsma, M., Lie, J.T., Dapena, I., Oellerich, S., Melles, G.R.J., 2018. Improving the success rate of human corneal endothelial cell cultures from single donor corneas with stabilization medium. Cell Tissue Bank. 19, 9–17.
Ting, D.S.J., Peh, G.S.L., Adnan, K., Mehta, J.S., 2022. Translational and regulatory challenges of corneal endothelial cell therapy: a global perspective. Tissue Eng. B Rev. 28, 52–62.
Ueno, M., Asada, K., Toda, M., Nagata, K., Sotozono, C., Kosaka, N., Ochiya, T., Kinoshita, S., Hamuro, J., 2016. Concomitant evaluation of a panel of exosome proteins and MiRs for qualification of cultured human corneal endothelial cells. Invest. Ophthalmol. Vis. Sci. 57, 4393–4402.
van Essen, T.H., Roelen, D.L., Williams, K.A., Jager, M.J., 2015. Matching for Human Leukocyte Antigens (HLA) in corneal transplantation - to do or not to do. Prog. Retin. Eye Res. 46, 84–110.
Walckling, M., Waterstradt, R., Baltrusch, S., 2020. Collagen remodeling plays a pivotal role in endothelial corneal dystrophies. Invest. Ophthalmol. Vis. Sci. 61, 1.
Wongvisavavit, R., Parekh, M., Ahmad, S., Daniels, J.T., 2021. Challenges in corneal endothelial cell culture. Regen. Med. 16, 871–891.

Zhang, Z.H., Miao, Y.Y., Ke, B.L., Liu, K., Xu, X., 2018. LY2109761, transforming growth factor β receptor type I and type II dual inhibitor, is a novel approach to suppress endothelial mesenchymal transformation in human corneal endothelial cells. Cell. Physiol. Biochem. : Int. J. Exp. Cell. Physiol., Biochem., Pharmacol. 50, 963–972.
Zhu, C., Joyce, N.C., 2004. Proliferative response of corneal endothelial cells from young and older donors. Invest. Ophthalmol. Vis. Sci. 45, 1743–1751.
Zhu, C., Rawe, I., Joyce, N.C., 2008. Differential protein expression in human corneal endothelial cells cultured from young and older donors. Mol. Vis. 14, 1805–1814.
Zhu, Y.-T., Chen, H.-C., Chen, S.-Y., Tseng, S.C.G., 2012. Nuclear p120 catenin unlocks mitotic block of contact-inhibited human corneal endothelial monolayers without disrupting adherent junctions. J. Cell Sci. 125, 3636–3648.